HHS Public Access

Author manuscript

J Immunol. Author manuscript; available in PMC 2022 December 15.

Published in final edited form as:

J Immunol. 2021 December 15; 207(12): 3122–3130. doi:10.4049/jimmunol.2001152.

Leptin Augments Anti-Tumor Immunity in Obesity by Repolarizing Tumor-Associated Macrophages

Stephanie O. Dudzinski[*,^], **Jackie E. Bader**[†,^], **Kathryn E. Beckermann**[‡,†], **Kirsten L. Young**[†,‡], **Rachel Hongo**[‡], **Matthew Z. Madden**[‡], **Abin Abraham**[§], **Bradley E. Reinfeld**[†], **Xiang Ye**[†], **Nancie J. MacIver**[¶], **Todd D. Giorgio**[*,‖,#], **Jeffrey C. Rathmell**[†,‖]

[*]Department of Biomedical Engineering, Vanderbilt University, Nashville, TN, 37232

[†]Department of Pathology, Microbiology, and Immunology, Vanderbilt University Medical Center, Nashville, TN, USA 37232

[‡]Department of Medicine, Division of Hematology/Oncology, Vanderbilt University Medical Center, Nashville, TN, USA 37232

[§]Department of Medicine, Division of Medical Genetics, Vanderbilt University Medical Center, Nashville, TN, USA 37232

[¶]Department of Pediatrics, Duke University Medical Center, Durham, NC 27710

[‖]Vanderbilt Center for Immunobiology, Vanderbilt University Medical Center, Nashville, TN 37232

[#]Department of Chemical and Biomolecular Engineering, Vanderbilt University, Nashville, TN 37232

Abstract

While obesity can promote cancer, it may also increase immunotherapy efficacy in what has been termed the obesity-immunotherapy paradox. Mechanisms of this effect are unclear, although obesity alters key inflammatory cytokines and can promote an inflammatory state that may modify tumor infiltrating lymphocytes (TIL) and tumor associated macrophage (TAM) populations. To identify mechanisms by which obesity affects anti-tumor immunity, we examined changes in cell populations and the role of the pro-inflammatory adipokine leptin in immunotherapy. Single cell RNAseq revealed that obesity decreased TIL frequencies and flow cytometery confirmed altered macrophage phenotypes with lower expression of iNOS and MHCII in tumors of obese animals. When treated with anti-PD-1 antibodies, however, obese mice had a greater absolute decrease in tumor burden than lean mice and a repolarization of the macrophages to inflammatory M1-like phentoypes. Mechanistically, leptin is a pro-inflammatory adipokine that is induced in obesity and may mediate enhanced anti-tumor immunity in obesity. To directly test the effect of leptin on tumor growth and anti-tumor immunity, lean mice were treated with leptin and tumors were observed over time. Treatment with leptin, acute or chronic, was sufficient to enhance anti-tumor

Address Correspondence to Todd D. Giorgio, todd.d.giorgio@vanderbilt.edu, or Jeffrey C. Rathmell, jeff.rathmell@vumc.org.
[^]Contributed equally

Author Contributions: SOD and JEB designed and performed the experiments, analyzed the data, and wrote the manuscript. TDG and JCR designed experiments and wrote the manuscript. KEB performed experiments and wrote the manuscript. NJM designed experiments. KLY, MZM, JEB, BER, XY, and RH performed experiments and performed data analysis. MZM, JEB, and AA analyzed data and created figures.

efficacy similar to anti-PD-1 checkpoint therapy. Further, leptin and anti-PD-1 co-treatment may enhance anti-tumor effects consistent with an increase in M1-like TAM frequency compared to non-leptin treated mice. These data demonstrate that obesity has dual effects in cancer through promotion of tumor growth while simultaneously enhancing anti-tumor immunity through leptin-mediated macrophage reprogramming.

Introduction

Obesity is a risk factor for at least 13 different types of cancer, and in the United States 36.2% of adults are obese (1). It is estimated that obesity is the cause of 14% and 20% of cancer deaths in men and women, respectively (2, 3). Obesity is correlated with the highest relative risk of development in intestinal cancers, such as esophageal, stomach and colorectal (2). Along with an increased risk of developing cancer, obese patients also have worse outcomes in regards to response to surgery, traditional chemotherapy, and radiation therapy treatments (4). Studies investigating the efficacy of immunotherapy in obese patient and mouse models have indicated that obesity can improve immunotherapy efficacy, but the complete mechanism for this is not yet understood (5, 6).

In obese patients, chronic lipid and nutrient overload can lead to increased inflammation in adipose tissue that promotes the constellation of pathologies termed the metabolic syndrome (7). Even prior to overt conditions of the metabolic syndrome such as type II diabetes or cardiovascular disease, immunity and immune responses are altered and impaired, and these immune changes are a predisposition for cancer development (8). Lean adipose tissue contains numerous anti-inflammatory cells including alternatively activated (M2) macrophages, T_H2 T cells and T Regulatory T cells (9). However, as adipocytes increase in size and quantity in obesity, they begin to secrete inflammatory adipokines and cytokines including leptin, tumor necrosis factor-α (TNF-α), interleukin-6 (IL-6), and monocyte chemotactic protein (MCP-1). Leptin, TNF-α, and IL-6 induce local and systemic inflammation and are known to be elevated in colon cancer (10, 11). Leptin and MHCII expression by adipocytes and myeloid cells, respectively, skew and activate T_H1 cells, and the T_H1 and $CD8^+$ T cells secrete elevated levels of interferon-γ (IFN-γ), further increasing adipose tissue inflammation (9). In obesity, macrophages are recruited through MCP-1 and TNF-α, and the elevated IFN-γ in adipose tissue promotes a shift towards a classically activated/inflammatory (M1) macrophage phenotype with increased MHCII expression and pro-inflammatory cytokine expression. Obesity also triggers intracellular pathways that upregulate cyclo-oxygenase-2 (COX2), signal transducer and activator of transcription 3 (STAT3) and nuclear factor-κB (NF-κB) pathways, which increase inflammation, cellular proliferation, and anti-apoptotic proteins (10, 12, 13). As metabolic syndrome develops, the concomitant high glucose concentrations further promote a pro-tumor microenvironment by activating Hif1α, and hyperinsulinemia further promotes cell growth and anti-apoptotic proteins (13). Additionally, excess inflammation is involved in the epithelial-to-mesenchymal transition, which can increase cellular metastatic potential and genomic instability, resulting in increased DNA damage and mutation load (10). Obesity induces local adipose tissue and systemic inflammation through a multitude of mechanisms that increases the risk of cancer development.

While inflammation can promote cancer cell survival and tumor progression, these chronic immune changes also impact and suppress adaptive, and potentially, anti-tumor immunity. While obese adipose tissue macrophages have pro-inflammatory “M1” characteristics, the phenotype of tumor-associated macrophages (TAMs) is not the same as that of the adipose tissue macrophages (14). M1-like macrophages have anti-tumor properties via production of pro-inflammatory cytokines and nitric oxide, while M2-like macrophages have immunosuppressive properties which result in a pro-tumor function (15). Tumor-associated macrophages (TAMs) usually make up the greatest portion of immune cells in tumors, and these macrophages typically have an M2-like phenotype that supports tumor growth and inhibits anti-tumor immune cells (16–18). Monocytes are recruited to tumors through the chemokines CCL2, CCL5, vascular endothelial growth factor (VEGF), and colony stimulating factors (GM-CSF and M-CSF)(19). The recruited monocytes then mature into M2-polarized macrophages due to the intratumoral cytokines TGFβ, IL-6, and IL-10 (20). TAMs also promote tumor progression and invasion by secreting matrix metalloproteinases and cathepsins that degrade extracellular matrix (ECM) proteins (18). Blood vessels needed for tumor progression are supported through TAM production of TGFβ and VEGF (17). Due to these pro-tumor functions, the majority of cancers have an association between high TAM density and poor patient prognosis (21). Gene set enrichment studies have demonstrated that ECM in obese patients polarizes macrophages to a stronger M2-like phenotype than that of ECM from lean patients (14).

Checkpoint inhibitor therapies work through blocking negative regulatory receptors. For example, the use of an antibody to PD-1 recovers the “exhausted” T-cell function and leads to subsequent tumor cell death (22). TAMs also express PD-1 that negatively correlates with anti-tumor function (23). The administration of anti-PD-1 (αPD-1) *in vivo* also improves macrophage anti-tumor function and reduces tumor growth (23). Immune checkpoint blockade treatment enhances survival for some patients, but clinical trials have demonstrated that efficacy of αPD-1 is limited with approximately one-quarter to one-third of patients showing a partial or complete response (24). To date there is no proven biomarker to predict response in many tumor types. While studies have focused predictive models using tumor-associated factors, such as T cell infiltration, PD-1 or PD-L1 expression, and mutation burden, fewer studies have focused on patient-associated factors such as age, smoking habits, diet composition, and body mass index (BMI). Studies investigating the effects of obesity on immunotherapy efficacy have largely focused on T cell phenotyping, identifying that obesity induces increased immune checkpoint blockade markers on T cells (5). However, the mechanism of how obesity affects immunotherapy remains unknown, especially with respect to the roles of immune cells other than T cells such as macrophages. Given the importance of TAMs in tumor progression, the potential for αPD-1 treatments to restore macrophage anti-tumor function, and the association of a stronger “M2” phenotype in obesity, we hypothesize that the macrophages will play a significant role for immunotherapy efficacy in obesity.

Here we investigated how obesity-induced inflammation contributes to differences in the tumor immune microenvironment and may alter immunotherapy efficacy in diet-induced obesity (DIO). Through single cell RNA sequencing we observed differences in the tumor immune cell landscape that revealed a diet effect primarly involving tumor myeloid cells.

Using flow cytometry, we demonstrate that TAM phenotypes change significantly with immunotherapy treatment in obese, but not lean mice. This effect appeared mediated, in part, by elevated levels of the adipokine, leptin, which was sufficient to enhance M1-like macrophage polarization. Interestingly, treatment of lean mice with leptin alone was sufficient to reduce tumor growth. Obesity plays dual roles by both promoting tumor progression and sensitizing to immunotherapy through elevated levels of leptin, which can alter TAM polarization to enhance anti-tumor immunity.

Materials and Methods

Mice

Mice were housed in pathogen-free facilities in ventilated cages with 5 animals per cage. All mouse studies and procedures were performed under Institutional Animal Care and Utilization Committee (IACUC)-approved protocols from Vanderbilt University. C57BL/6 mice were obtained from the Jackson laboratory at 3 weeks of age. Diet-induced obese (DIO) and control mice were generated by feeding mice with an open-source purified diet consisting of either 60% fat (D12492 Research Diets, Inc) or continued on standard housing diet (LabDiet Rodent 5001) with 10.7% fat when mice were 5 weeks old, respectively. Mice were maintained on their respective diet for 12 weeks before initiating tumor growth studies.

Leptin measurements

Plasma leptin concentrations were measured using Leptin Mouse Quantikine ELISA kit as per the manufacturer's instructions (R&D systems).

Tumor cell line and treatment

The murine colorectal cell line MC38-CEA1 was purchased from Kerafast. C57BL/6 mice were injected subcutaneously in the right flank with 1×10^5 MC38-CEA1 cells in 200 μL PBS for the tumor growth studies in DIO and lean mice and 2.5×10^5 MC38-CEA1 cells in 200 μL PBS for immunotherapy and leptin studies. Tumors were measured with digital calipers every 2–3 days, and tumor volume was calculated as length (mm) × width^2 (mm) × 0.5. In immunotherapy studies, C57BL/6 MC38-CEA tumor bearing mice received either intraperitoneal injections of 200 μg anti-mouse PD-1 antibody (RMP1–14, BioXCell) in 200 μL PBS or 200 μg rat IgG2a isotype control (2A3, BioXCell) in 200 μL PBS on days 5, 7, 9, 11, 13, and 15.

For leptin studies, recombinant leptin (R&D Systems) was injected at a 1 μg/g body weight concentration in 200 μL of PBS, twice daily while control mice received 200 μL of PBS. All leptin experiments were initiated when mice were 5 weeks old. Chronic leptin experiments started leptin treatments two weeks before tumor injection and continued treatments throughout tumor growth. Acute leptin experiments started leptin treatments on day 5 post-tumor injection.

Tumor Dissociation

To prevent tumors from growing past the 2 cm limit per the IACUC protocol, tumors were collected on day 16 days post-injection. Fresh tumors were first processed with

mechanical dissociation, followed by enzymatic digestion with 9.28 mg/mL DNase I (Sigma D5025) and 0.1 g/mL collagenase IA (Sigma C2674), for 1 hour at room temperature using a dissociator (Miltenyi) with gentleMACS C-tubes. To remove calcium, cells were resuspended for 5 min in HBSS without calcium or magnesium (Gibco), then resuspended in 5 mM of ethylenediaminetetraacetic acid (EDTA) for 30 min at room temperature. Next, cells were passed through a 70 μm filter before ammonium-chloride-potassium (ACK) lysing buffer (KD Medical Inc) was added to remove red blood cells before flow cytometry. Immediate staining was performed for surface marker expression analysis by flow cytometry.

Mouse flow cytometry

One million cells of each tumor or spleen were transferred to a 96-well round-bottom, micro test plate and pelletized at 1500 rpm (524 g) for 5 min (Beckman-Coulture Allegra X-14 Centrifuge). A fixable viability dye (eBioscience, eFluor 780) was used to identify live cells. The following antibodies were used for surface staining: CD45 BV510 (Biolegend, Clone: 30-F11), CD3 FITC (Thermofisher, Clone: 17A2), CD4 PECy5 (Thermofisher, Clone GK1.5), CD8a eFluor 450 (Thermofisher, Clone: 53–6.7), CD279 (PD-1) APC (Thermofisher, Clone: J43), CD279 (PD-1) PE (Biolegend, Clone: RMP1–14), CD44 PECy7 (Thermofisher, Clone: IM7), Foxp3 PE (Thermofisher, Clone: FJK-16S), CD11b eFluor 450 (Thermofisher, Clone: M1/70), F4/80 FITC (Thermofisher, Clone: BM8), CD206 APC (Biolegend, Clone: C068C2), CD86 PE (BD Biosciences, Clone: GL1), iNOS2 PE (Thermofisher, Clone: CXNFT), I-A/I-E (MHCII) (Biolegend, Clone: M5/114.15.2). Briefly, cells were treated with Fc blocking antibodies (TruStain FcX Biolegend) for 10 min at 4 °C followed by cell surface antibodies in FACS Buffer (PBS with 2% FBS) for 30 min at 4 °C. For T cell intracellular staining the FoxP3/Transcription Factor Staining kit (ThermoFisher) was used. The Cytofix/Cytoperm Fixation and Permeabilization Solution Kit (BD Biosciences) was used for macrophage intracellular staining. Cells were pelletized at 1500 rpm (524 g) for 5 min before re-suspending in 200 μL of FACS Buffer. Expression of immune cell surface markers was measured by fluorescence cytometry (MACSQuant, Miltenyi Biotec) and analyzed by FlowJo software (Tree Star Inc.). To select immune cells, live cells were first gated on a fixable viability dye, then a CD45+ cell gate was applied before selecting immune cell subtypes (Supplementary Figure 1A). Some tumor samples did not have enough cells for multiple flow cytometry panels.

Bulk TAM mRNA transcript analysis

Mice were subcutaneously injected with 250,000 MC38-CEA1 cells in the right flank on day 0, intraperitoneally injected with 250 mcg anti-PD1 antibody (clone RMP1–14, BE0146 Bio X Cell) or IgG control (clone 2A3, BE0089 Bio X Cell) on days 11 and 13, and euthanized on day 16. CD11b+ tumor cells were isolated from tumor single cell suspensions using CD11b Microbeads (Miltenyi 130–049-601) according to manufacturer's instructions. Then, cells were stained with the indicated surface markers and viability dye, and TAMs (live CD45+ CD11b+ F4/80 hi CD3− CD19− NKp46− Ly6C lo Ly6G−) were sorted on a BD FACSAria III cell sorter. RNA was isolated from TAMs using the Quick-RNA™ Microprep Kit (Zymo R1050) according to manufacturer's instructions. RNA transcripts were quantified using the NanoString nCounter Metabolic Pathways Gene Expression

Panel (XT-CSO-MMP1–12) according to manufacturer's instructions. Transcript levels were normalized to internal control housekeeping genes using the NanoString nSolver software.

To identify differentially expressed genes across diet (LFD and HFD) and treatment (anti-PD1 and IgG), we compared transcript counts in the treatment vs control group stratified by diet and HFD vs. LFD stratified by treatment. This resulted in four pairwise comparisons: 1) anti-PD1+HFD vs. IgG+HFD, 2) anti-PD1+LFD vs. IgG+LFD, 3) HFD+anti-PD1 vs. LFD+anti-PD1, and 4) HFD+IgG vs. LFD+IgG. Each condition (diet + treatment combination) had three replicates with Nanostring transcript counts. The transcripts counts were normalized using internal housekeeping genes such that the minimum value was 1. After estimating the dispersion (variance of transcript counts) using the function "estimateDisp", differential expression between conditions was evaluated using a likelihood ratio test for a negative binomial generalized log-linear model. We considered transcripts with a false discovery rate < 10% as being differentially expressed. For differentially expressed transcripts in any of the four pairwise comparisons, we plotted the transcript count as a heatmap and grouped them using hierarchical clustering. Differential expression was evaluated using the package "edgeR" (version 3.28.1) within the statistical computing software R (version 3.6.3). Heatmap and clustering was performed using the package 'seaborn' (version v0.11.0) using Python3.6.

Single-cell RNA sequencing

8-week-old C57BL/6 male mice were fed ad libitum with either a 10% kcal from fat (low fat) diet or a 45% kcal fat (high fat) diet (Research Diets D12450H and D12451, respectively). Following 28 weeks of diet treatment, mice were injected subcutaneously with 2×10^5 murine MC38 (Kerafast) cells. Tumors were collected on day 20 post injection then mechanically and enzymatically digested using mouse tumor digestion kit (Miltenyi) following manufacturer's instructions. Tumor-infiltrating leukocytes were sorted by positive selection using CD45+ microbeads (Miltenyi Biotec) from dissociated tumors for single-cell analysis. CD45+ cells were further enriched for live cells using a dead cell removal kit (Miltenyi Biotec) Cells were diluted with trypan blue and counted using a hemocytometer. Three tumors possessing the median weights were pooled together for each treatment group. Pooled samples were resuspended at 1×10^6 cells/mL in PBS plus 0.4% BSA with a target of 20,000 live cells loaded onto the Chromium Controller (10X genomics) and processed according to the manufacturer's instructions. Sequencing was performed on the Illumina NovaSeq 6000 targeting 50,000 reads per cell for the 5' assay. The raw data (FASTQ files) were demultiplexed and processed using the velocyto (version 0.17.17) to generate gene expression matrix as loom files.

Data pre-processing, normalization, integration, and clustering were performed within scanpy (version 1.7.1). Briefly, the gene expression matrix for each sample was filtered by keeping cells in with more than 200 and less than 4000 genes were detected and genes that were detected in more than 3 cells. Cells with mitochondrial genes representing greater than 10% percent of the transcripts were also removed. The matrix for each sample was integrated using a MNN (mutual nearest neighbor) algorithm with 4002 highly variable genes (highly variable genes in at least two samples). LFD and HFD samples were merged

into one matrix. Clustering performed via Leiden which identified 20 clusters that were then annotated using SingleR and manually confirmed. Violin plots of genes were made with scanpy(25). Data are available online at GEO under https://www.ncbi.nlm.nih.gov/geo/query/acc.cgi?acc=GSE179936.

Statistics

Prism software (GraphPad Software Inc.) was used to create graphs and conduct statistical analyses. Data were expressed as mean ± standard error of the mean (s.e.m.). For analysis of three or more groups, one-way analysis of variance (ANOVA) tests were performed with Tukey post-hoc test. For tumor growth, a two-way analysis of variance (ANOVA) was used. The differences between two test groups was performed using the Mann-Whitney test. Differences between more than two test groups was determined using a one-way analysis of variance (ANOVA). For scRNA sequencing violin plot a students t test was performed and adjusted using benjamini-hochberg procedure. p values were considered statistically significant if $p < 0.05$.

Results

Obesity Elevates Basal T-Cell Stimulation

Spleens from non-tumor bearing mice were characterized to identify baseline differences in systemic immune profiles between DIO and lean mice. Five-week old C57BL/6 male mice were fed either a low-fat diet (LFD) or high fat diet (HFD) for 12 weeks, over which time the DIO mice gained significantly greater weight than lean mice (Figure 1A). Systemic inflammation was quantified with markers of T cell activation and exhaustion (26, 27). There was a trend for fewer $CD8^+$ T cells in the spleens of DIO mice (Supplementary Figure 1 A,B). However, a higher frequency of $CD8^+$ T cells expressed elevated levels of the CD44 marker of activation among DIO mouse splenic T cells compared to lean mouse splenic T cells (Figure 1B). The chronic inflammatory state and activation of immune cells in obesity may upregulate exhaustion markers including PD-1. In contrast to CD44, PD-1 was not significantly upregulated on splenic $CD8^+$ T cells in DIO compared to LFD mouse splenic T cells (Supplementary Figure 1C). Together, these data support previous findings and suggest that obesity induces a systemic chronically stimulated T cell phenotype (5). The presence of activation and checkpoint markers on T cells in DIO mice suggests that the obese mice have an elevated inflammatory profile that may influence tumor growth and response to immunotherapy.

Obesity Increases Tumor Growth and Decreases Anti-Tumor Inflammation

After establishing that DIO can shift T cells to more activated phenotypes, we tested how obesity affected tumor-infiltrating immune cells. The MC38-CEA1 colon cancer model was chosen because it is compatible with the C57BL/6 DIO model and is responsive to treatment with anti-PD-1 immunotherapy (28). As expected, MC38-CEA1 subcutaneous tumors grew significantly larger in DIO mice compared to lean mice (Figure 1C, Supplemental Figure 1D). Despite increased frequencies of $CD44^+$ $CD8^+$ T cells in spleens of non-tumor bearing DIO mice, tumor infiltrating $CD44^+$ $CD8^+$ T cells were unchanged or trended toward decreased absolute cell numbers within tumors of HFD-fed animals compared to

LFD-fed (Figure 1D). These tumor-infiltrated T cells expressed similar levels of PD-1 but an increased frequency expressed high levels of CD44 (Supplemental Figure 1E). Tumor macrophages, identified as CD11b and F480 double positive cells, were similarly unchanged or trending toward a decrease in total numbers in tumors from HFD-fed mice (Figure 1E). Phenotypically, however, DIO macrophages appeared to have decreased key M1-like characteristics (29). TAMs from HFD-fed mice expressed lower levels of iNOS and PD-L1 (Figure 1F, Supplemental Figure 1F). The composition of myeloid cells was also altered as fewer monocytic ($Ly6C^+CD11b^+$) and granulocytic ($Ly6G^+CD11b^+$) myeloid derived suppressor cells were present in the spleens of DIO tumor-bearing obese mice (Supplementary Figure 1G). The non-hematopoietic cells within the tumors, which were comprised largely of cancer cells, were also altered and had reduced expression of PD-L1 (Supplemental Figure 1H). Given the role of IFNγ to induce PD-L1, these data are consistent with a heightened systemic inflammation, but with intra-tumoral inflammation reduced in HFD relative to that of LFD.

To better dissect the effects of DIO on the tumor immune landscape, single-cell RNAseq (scRNAseq) of the MC38 tumors was performed. Leukocytes were characterized by CD45 expression and isolated from tumors in LFD and HFD mice for scRNAseq. Data were analyzed using SingleR to identify cell populations based on gene signatures (Figure 2A). Most notable was the altered myeloid populations of HFD-fed, DIO tumors that revealed a decrease within the monocyte-identified clusters in addition to an increase within the macrophage-identified clusters (Figure 2B,C). The macrophage-identified TAMs had reduced *CD274* (PD-L1), *Tgfb* and *Tnfa* expression in DIO mice (Figure 2D, Supplementary Figure 2). TAMs from DIO mice also had decreased and *Il10* gene expression compared to TAMs from lean mice and appeared metabolically more quiescent, with reduced gene expression of glycolytic genes including *Slc2a1* and *Ldha* and the metabolic regulatory gene *Egln3* (PHD3) while the fatty acid oxidation gene *Cpt1a* was increased (Supplementary Figure 2). Tumor-resident $CD8^+$ T cells decreased in frequency in DIO mice and had reduced expression of PD-1 and Granzyme B (Figure 2C,D). Expression of inflammatory cytokines including *Ifng* and *Tnfa* were not significantly different in $CD8^+$ T cells within DIO tumors compared to tumors from lean mice (Supplemental Figure 2). Metabolic genes including, *Cpt1a*, *Slc2a1*, *Ldha* and *Egln3* did not significantly differ in $CD8^+$T cells from DIO tumors compared to lean mice. These results are consistent with other recent findings that reported reduced $CD8^+$ T cells and lower levels of glycolysis genes and *Egnl3* in tumors of obese mice (30). Our data further highlight substantial shifts in TAM populations in tumors of mice with DIO.

DIO Mice Experience Greater Magnitude Responses and Macrophage Reprogramming with Immunotherapy

Given the systemic and intratumoral effects of DIO on immune cell populations, we next tested the effects of obesity on immunotherapy efficacy. Lean and obese mice with subcutaneous MC38-CEA1 tumors were treated with anti-PD-1 antibodies starting on day 5 post-injection and continued every two days until sacrifice on day 16. Anti-PD-1 antibody treatment reduced tumor volume in both obese and lean mice, but the decrease in tumor volume was larger for the obese mice (Figure 3A, Supplemental Figure 3A). Of note,

although the obese mice had a larger mean decrease in volume than the lean mice, the percent volume change of treated to control was not different between obese and lean mice (Supplemental Figures 3B,C). Although tumors were reduced in size with anti-PD-1 treatment, we did not observe an increase in tumor infiltrating $CD8^+$ T cells producing IFNγ or in numbers of TAMs (Supplemental Figure 3D,E). The phenotype of TAMs within treatment groups, however, did change. Tumors from the obese group treated with IgG only had a significantly smaller fraction of TAMs expressing MHCII than tumors from lean mice (Figure 3B). This was rescued, however, following treatment with anti-PD-1 as TAMs in obese mice regained MHCII compared to IgG controls. Gene expression analysis identified significant alterations in TAM from obese anti-PD-1 treated versus control IgG-treated mice that did not occur in lean mice (Figure 3C, Supplemental Figure 3F). Of note, pro-inflammatory M1-associated genes were increased in HFD anti-PD-1 TAMs including *Nos2*, *Il6*, and *Ccl5*. *CD274* (which encodes PD-L1), *Arg1*, and *Kynu*, were also upregulated, to suggest a generally activated and mixed phenotype with some characteristics of M2-like macrophages. Additionally, glucose transporter, *Slc2a1* (Glut1) and phagocytosis associated gene *Fcrb1* were increased in TAMs from anti-PD-1 treated obese mice compared to vehicle treated obese mice or lean mice. These findings show that anti-PD-1 can promote activation and reprogramming of TAMs and this effect is particularly evident in obesity.

Leptin Decreases Tumor Growth and Promotes TAM Repolarization

Leptin is an adipokine elevated in obesity that is correlated with elevated PD-1 levels on $CD8^+$ T cells and reported to polarize macrophages to an M1-like phenotype (5, 31–35). The effects of leptin on TAM polarization, however, are uncertain. Leptin was significantly elevated in the plasma of DIO mice compared to LFD mice (Figure 4A). The ability of leptin to induce M1-macrophage polarization was analyzed without the additional immune and hormone changes generated in DIO models by exogenous leptin injections in young, lean mice. Previous studies have shown that leptin-receptor positive cancer cell lines can exhibit increased proliferation with exogenous leptin (36). MC38 cells, however, do not express leptin receptors and provided an opportunity to study the effects of leptin on immune cells in the tumor microenvironment (37). Mice received leptin or PBS control injections intraperitoneally twice a day for two weeks before injecting the mice subcutaneously with MC38-CEA1 colon cancer cells. Consistent with leptin as a satiety signal, mice lost weight during the first week of treatment although much of this weight was regained during the second week of treatment (Supplemental Figure 4A)(38). Leptin injections were continued throughout the experiment. As anticipated, leptin had systemic effects to enhance inflammatory phenotypes, with increased expression of CD86 and MHCII in splenic macrophages (Supplemental Figures 4B, C). Mice treated with leptin also had significantly smaller tumors than PBS-control treated mice to demonstrate that elevated leptin is sufficient to reduce overall tumor growth (Figure 4B, Supplemental Figure 4D). Similar to elevated inflammatory states for splenic macrophages, leptin treatment also reversed some obese-mediated inhibitory effects on TAMs and led to greater expression of MHCII and a trend to increase CD86 on DIO TAMs, suggesting that leptin induced a more M1-like phenotype (Figure 4C).

Acute Leptin Treatments Cooperate with PD-1 blockade Immunotherapy and Repolarize TAMs to M1 Phenotypes

Given the proinflammatory effects of chronic leptin treatments, we next tested if leptin could act as an immunotherapy to protect against established tumors. Leptin treatments were initiated alone or simultaneously with PD-1 blockade immunotherapy treatment on day 5 post injection. The same MC38-CEA1 tumor model, immunotherapy, and leptin treatment dosing was used as in other experiments for this study. The leptin IgG, PBS anti-PD-1, and leptin anti-PD-1 treatment groups all had significantly smaller tumors than the control PBS IgG treated group, with leptin alone leading to comparable reductions in tumor size as anti-PD-1 alone (Figure 5A, Supplemental Figure 4E). The tumor growth curves exhibit a trend for smallest tumor volume in the leptin and anti-PD-1 co-treatment mice. The anti-PD-1 monotherapy and leptin with anti-PD-1 co-treatment significantly decreased frequency of TAMs (Figure 5B, Supplemental Figure 4F). $Ly6C^{+}CD11b^{+}$ Monocytic MDSCs were also decreased with immunotherapy (Supplemental Figure 4G). The remaining TAMs in the leptin and anti-PD-1 co-treatment group, however, had the highest M1-like markers MHCII and iNOS2 (Figure 5C, D). Interestingly, anti-PD1 was more effective to repolarize macrophages to upregulate MHCII while leptin was more effective to induce iNOS suggesting a potential cooperative reprogramming of macrophages to more inflammatory states. These data suggest that while obesity reduces macrophages inflammatory states within tumors, leptin is sufficient to polarize TAMs to more inflammatory states, which may contribute to the obesity paradox of increased efficacy of immunotherapy.

Discussion

Our findings demonstrate a correlation between macrophage repolarization and enhanced immunotherapy efficacy in obese mice and suggest that leptin contributes to this effect. Leptin is sufficient to reduce tumor size and may also provide a novel approach to immunotherapy. Similar to previous findings, obese mice experienced a greater decrease in overall tumor volume than lean mice following immunotherapy (5, 6). While the mechanism by which obesity both promotes tumors and enhances immunotherapy responses remains uncertain, our flow cytometric and single cell RNAseq analyses point to significant changes in TAM populations in obesity that are reversed with immunotherapy. These findings are consistent with recent retrospective clinical studies identified that macrophage polarization improved prediction of immunotherapy efficacy (5, 39). Further, our data point to leptin as an inflammatory adipokine that can act as a new immunotherapy alone or combinational therapy to augment the effectiveness of PD-1 checkpoint blockade.

TAMs can play complex roles in tumor microenvironments and reflect a spectrum of phenotypes. TAMs can display phenotypes of classically activated M1-like or alternatively activated M2-like macrophages that can increase tumor initiation, progression, and metastasis rates (15, 40). We found a shift in TAM phenotypes with HFD to a weaker M1-like state compared to TAMs from lean control mice. Treatment with anti-PD-1 reversed this effect and TAMs from DIO mice treated with anti-PD-1 had similar M1-like phenotypes as the TAMs from lean mice. Interestingly, these anti PD-1 induced changes in macrophage polarization were most evident in obese animals. Anti-PD-1 therapy normalized TAM

polarization in obese and lean models despite the greater degree of dysregulated, M2-like polarization in TAMs of obese mice. The efficacy of M1-like TAMs in direct tumor cytotoxicity relative to their modulation of TIL cytotoxic activity in the tumor remains poorly understood, particulary in the context of obesity and immunotherapy. These shifting macrophage phenotypes may contribute to the obesity paradox by enhancing tumor growth in their native M2-like polarization while priming macrophages for more inflammatory states after immune checkpoint blockade treatment.

Although leptin is commonly known as an adipokine regulating appetite and fat storage, it has also been shown to activate the immune system and can be secreted in infections, autoimmune diseases, and obesity (11, 38). Leptin decreases the regulatory T cell population while promoting and activating the T_H1 phenotype of cells (11). T cells exposed to leptin will subsequently have increased activation markers and cytokine production (11). In macrophages, leptin promotes an M1-like phenotype with increased phagocytic function, iNOS expression, and secretion of TNF-α, IL-6, and IL-12 (31, 41). Studies at the intersection of leptin, obesity, and macrophages have primarily focused on modulation of adipose tissue macrophage inflammation. Leptin deficiency repolarizes pro-inflammatory adipose tissue macrophages to a M2-like phenotype (33). Our study tested if leptin can repolarize TAMs to a M1-like phenotype, subsequently decreasing tumor size, and potentially enhance immunotherapy efficacy as was observed in obese mice. Both T cells and macrophages express leptin receptors that activate STAT3 and STAT1 respectively, and eventually result in PD-1 upregulation (42). Others have studied targeted effects of leptin on TILs and the associated decrease in tumor burden, but our data suggest a role for leptin to repolarize macrophages in immunotherapy (43). Exogenous leptin treatment did decrease bodyweight during the initial weeks of treatment, which in principle may influence tumor growth indirectly. However, the majority of bodyweight was recovered at the time of tumor injection suggesting that any leptin alterations to food intake had stabilized. Chronic leptin-treated mice had significantly smaller tumors and an increased M1-macrophage phenotype. When combining leptin treatments with anti-PD-1 antibodies, the co-treated mice had the smallest tumors, the greatest decrease in TAM frequency, and the largest increase in M1-like polarization compared to monotherapy and control treated mouse tumors. Of note, elevated leptin in obesity can result in leptin resistance, and if exogenous leptin is provided to DIO mice, the macrophages do not polarize to an M1-like phenotype (44). DIO immunotherapy treated mice and the lean leptin and immunotherapy co-treated mice had a very similar immune profile compared to controls. In addition to assessing the effects of leptin on TAMs, it will also be important to consider the influence of leptin on cancer cells, as high leptin levels may also promote proliferation of some cancer types depending on expression of the leptin receptor(45).

Our data provide novel connections between obesity and leptin's effect on TAM modification with tumor progression and immunotherapy response. While obese mice possessed increased tumor burden and decreased M1-like phenotype of TAMs compared to lean mice, immunotherapy treatment in obese mice repolarizes the TAMs to an M1-like phenotype, which resulted in a larger decrease in tumor burden than in lean mice. Leptin may contribute to the increased M1-like macrophage polarization during anti-PD-1 antibody treatment of obese mice, as was observed in the experiments with exogenous

leptin delivery. Importantly, lean mice given anti-PD-1 treatments alone did not show evidence of macrophage repolarization, suggesting that leptin is necessary for macrophage repolarization during immune checkpoint blockade. Further studies are needed to identify the exact interactions between leptin, TAMs, and immunotherapy as well as investigate other types of immunosuppressive cells. Nevertheless, our data show a dual role for obesity to both promote tumor progression while sensitizing to immunotherapy through elevated levels of leptin, which was sufficient to alter TAM polarization and promote anti-tumor immunity. Additionally, we show that leptin treatment reduces tumor growth and leptin together with anti-PD-1 co-treatment may ehance these anti-tumor effects. These studies highlight the importance of leptin in TAMs and suggest that leptin plays a key role to augment repolarizing of TAMs to increase immunotherapy efficacy.

Supplementary Material

Refer to Web version on PubMed Central for supplementary material.

Acknowledgements:

We thank members of the Giorgio and Rathmell labs as well as Dr. Liza Makowski (University of Tennessee Health Sciences) for their input and constructive comments.

This work was supported by F30 CA224559 (SOD), K00 CA234920 (JEB), F30 CA239367 (MZM), F30 CA247202 (BER), T32 GM007347 (SOD, MZM, BER, AA), T32 DK101003 (SOD), R01 DK106090 (NJM), and R01 CA217987 (JCR). The Vanderbilt VANTAGE Core provided technical assistance for this work. VANTAGE is supported in part by CTSA Grant (5UL1 RR024975-03), the Vanderbilt Ingram Cancer Center (P30 CA068485), the Vanderbilt Vision Center (P30 EY08126), and NIH/NCRR (G20 RR030956). Flow sorting experiments were performed in the VMC Flow Cytometry Shared Resource and were supported by the Vanderbilt Ingram Cancer Center (P30 CA068485) and the Vanderbilt Digestive Disease Research Center (P30 DK058404).

Conflict of Interest: JCR is a founder, scientific advisory board member, and stockholder of Sitryx Therapeutics, a scientific advisory board member and stockholder of Caribou Biosciences, a member of the scientific advisory board of Nirogy Therapeutics, has consulted for Merck, Pfizer, and Mitobridge within the past three years, and has received research support from Incyte Corp., Calithera Biosciences, and Tempest Therapeutics.

Abbreviations used in this article:

DIO	extracellular matrix
ECM	diet induced obesity
HFD	high fat diet
LFD	low fat diet
PD-1	Programmed Cell Death Protein 1
PD-L1	Programmed Cell Death Protein Ligand 1
scRNAseq	single cell RNA sequencing
TAM	tumor associated macrophage
TIL	tumor infiltrating lymphocyte

References

1. Venegas O, and Mehrzad R. 2020. Prevalence and trends in obesity in the United States and affluent countries. In Obesity Elsevier. 19–41.
2. Secretan BL, Scoccianti C, Loomis D, and for R IA. on C. H. W. Group. 2016. Body Fatness and Cancer — Viewpoint of the IARC Working Group. N Engl J Med 375: 794–798. [PubMed: 27557308]
3. Calle EE, Rodriguez C, Walker-Thurmond K, and Thun MJ. 2003. Overweight, Obesity, and Mortality from Cancer in a Prospectively Studied Cohort of U.S. Adults. N Engl J Med 348: 1625–1638. [PubMed: 12711737]
4. Carmichael a R., and Bates T. 2004. Obesity and breast cancer: a review of the literature. Breast 13: 85–92. [PubMed: 15019686]
5. Wang Z, Aguilar EG, Luna JI, Dunai C, Khuat LT, Le CT, Mirsoian A, Minnar CM, Stoffel KM, Sturgill IR, Grossenbacher SK, Withers SS, Rebhun RB, Hartigan-O'Connor DJ, Méndez-Lagares G, Tarantal AF, Isseroff RR, Griffith TS, Schalper KA, Merleev A, Saha A, Maverakis E, Kelly K, Aljumaily R, Ibrahimi S, Mukherjee S, Machiorlatti M, Vesely SK, Longo DL, Blazar BR, Canter RJ, Murphy WJ, and Monjazeb AM. 2019. Paradoxical effects of obesity on T cell function during tumor progression and PD-1 checkpoint blockade. Nat. Med 25: 141–151. [PubMed: 30420753]
6. McQuade JL, Daniel CR, Hess KR, Mak C, Wang DY, Rai RR, Park JJ, Haydu LE, Spencer C, Wongchenko M, Lane S, Lee DY, Kaper M, McKean M, Beckermann KE, Rubinstein SM, Rooney I, Musib L, Budha N, Hsu J, Nowicki TS, Avila A, Haas T, Puligandla M, Lee S, Fang S, Wargo JA, Gershenwald JE, Lee JE, Hwu P, Chapman PB, Sosman JA, Schadendorf D, Grob JJ, Flaherty KT, Walker D, Yan Y, McKenna E, Legos JJ, Carlino MS, Ribas A, Kirkwood JM, Long GV, Johnson DB, Menzies AM, and Davies MA. 2018. Association of body-mass index and outcomes in patients with metastatic melanoma treated with targeted therapy, immunotherapy, or chemotherapy: a retrospective, multicohort analysis. Lancet Oncol. 19: 310–322. [PubMed: 29449192]
7. Iyengar NM, Gucalp A, Dannenberg AJ, and Hudis CA. 2017. Obesity and Cancer Mechanisms : Tumor Microenvironment and In fl ammation. J. Clin. Oncol 34: 4270–4277.
8. Hotamisligil GS 2017. Foundations of Immunometabolism and Implications for Metabolic Health and Disease. Immunity 47: 406–420. [PubMed: 28930657]
9. Deng T, Lyon CJ, Bergin S, Caligiuri MA, and Hsueh WA. 2016. Obesity, Inflammation, and Cancer. Annu. Rev. Pathol. Mech. Dis 11: 421–449.
10. Donohoe CL, Lysaght J, O'Sullivan J, and Reynolds JV. 2017. Emerging Concepts Linking Obesity with the Hallmarks of Cancer. Trends Endocrinol. Metab 28: 46–62. [PubMed: 27633129]
11. La Cava A 2017. Leptin in inflammation and autoimmunity. Cytokine 98: 51–58. [PubMed: 27916613]
12. Catrysse L, and van Loo G. 2017. Inflammation and the Metabolic Syndrome: The Tissue-Specific Functions of NF-κB. Trends Cell Biol. 27: 417–429. [PubMed: 28237661]
13. Taniguchi K, and Karin M. 2018. NF-κB, inflammation, immunity and cancer: coming of age. Nat. Rev. Immunol 18: 309–324. [PubMed: 29379212]
14. Springer NL, Iyengar NM, Bareja R, Verma A, Jochelson MS, Giri DD, Zhou XK, Elemento O, Dannenberg AJ, and Fischbach C. 2019. Obesity-Associated Extracellular Matrix Remodeling Promotes a Macrophage Phenotype Similar to Tumor-Associated Macrophages. Am. J. Pathol 189: 2019–2035. [PubMed: 31323189]
15. Lin Y, Xu J, and Lan H. 2019. Tumor-associated macrophages in tumor metastasis: biological roles and clinical therapeutic applications. J. Hematol. Oncol 12: 76. [PubMed: 31300030]
16. Malekghasemi S, Majidi J, Baghbanzadeh A, Abdolalizadeh J, Baradaran B, and Aghebati-Maleki L. 2020. Tumor-associated macrophages: Protumoral macrophages in inflammatory tumor microenvironment. Adv. Pharm. Bull 10: 556–565. [PubMed: 33062602]
17. Poh AR, and Ernst M. 2018. Targeting macrophages in cancer: From bench to bedside. Front. Oncol 8: 1–16. [PubMed: 29404275]
18. Vinogradov S, Warren G, and Wei X. 2014. Macrophages associated with tumors as potential targets and therapeutic intermediates. Nanomedicine 9: 695–707. [PubMed: 24827844]

19. Owen JL, and Mohamadzadeh M. 2013. Macrophages and chemokines as mediators of angiogenesis. Front. Physiol 4 JUL: 1–8. [PubMed: 23372552]
20. Zhou K, Cheng T, Zhan J, Peng X, Zhang Y, Wen J, Chen X, and Ying M. 2020. Targeting tumor-associated macrophages in the tumor microenvironment (Review). Oncol. Lett 20: 1–13. [PubMed: 32774475]
21. Larionova I, Cherdyntseva N, Liu T, Patysheva M, Rakina M, and Kzhyshkowska J. 2019. Interaction of tumor-associated macrophages and cancer chemotherapy. Oncoimmunology 8: 1–15.
22. Jiang Y, Li Y, and Zhu B. 2015. T-cell exhaustion in the tumor microenvironment. Cell Death Dis. 6: e1792–e1792. [PubMed: 26086965]
23. Gordon SR, Maute RL, Dulken BW, Hutter G, George BM, McCracken MN, Gupta R, Tsai JM, Sinha R, Corey D, Ring AM, Connolly AJ, and Weissman IL. 2017. PD-1 expression by tumour-associated macrophages inhibits phagocytosis and tumour immunity. Nature 545: 495–499. [PubMed: 28514441]
24. I G, A. H. A. Jr, I. M., and S. C. 2015. Immunology and breast cancer: Toward a new way of understanding breast cancer and developing novel therapeutic strategies. Clin. Adv. Hematol. Oncol 13: 372–382. [PubMed: 26352893]
25. Aibar S, González-Blas CB, Moerman T, Huynh-Thu VA, Imrichova H, Hulselmans G, Rambow F, Marine J-C, Geurts P, Aerts J, van den Oord J, Atak ZK, Wouters J, and Aerts S. 2017. SCENIC: single-cell regulatory network inference and clustering. Nat. Methods 14: 1083–1086. [PubMed: 28991892]
26. Ben-Neriah Y, and Karin M. 2011. Inflammation meets cancer, with NF-κB as the matchmaker. Nat. Immunol 12: 715–723. [PubMed: 21772280]
27. Didonato JA, Mercurio F, and Karin M. 2012. NF-κB and the link between inflammation and cancer. Immunol. Rev 246: 379–400. [PubMed: 22435567]
28. Ngiow SF, Young A, Jacquelot N, Yamazaki T, Enot D, Zitvogel L, and Smyth MJ. 2015. A Threshold Level of Intratumor CD8+ T-cell PD1 Expression Dictates Therapeutic Response to Anti-PD1. Cancer Reseach 75: 3800–3811.
29. Xue Q, Yan Y, Zhang R, and Xiong H. 2018. Regulation of iNOS on Immune Cells and Its Role in Diseases. Int. J. Mol. Sci 19: 3805.
30. Ringel AE, Drijvers JM, Baker GJ, Catozzi A, García-Cañaveras JC, Gassaway BM, Miller BC, Juneja VR, Nguyen TH, Joshi S, Yao C-H, Yoon H, Sage PT, LaFleur MW, Trombley JD, Jacobson CA, Maliga Z, Gygi SP, Sorger PK, Rabinowitz JD, Sharpe AH, and Haigis MC. 2020. Obesity Shapes Metabolism in the Tumor Microenvironment to Suppress Anti-Tumor Immunity. Cell 1848–1866. [PubMed: 33301708]
31. Loffreda S, Yang S, Lin H, Karp C, Brengman M, Wang D, Klein A, Bulkley G, Bao C, Noble P, Lane M, and Diehl A. 1998. Leptin regulates proinflammatory immune responses. FASEB J. 12: 57–65. [PubMed: 9438411]
32. Castoldi A, De Souza CN, Saraiva C NO??mara, and Moraes-Vieira PM. 2016. The macrophage switch in obesity development. Front. Immunol. 6: 1–11.
33. Zhou Y, Yu X, Chen H, Sjöberg S, Roux J, Zhang L, Ivoulsou AH, Bensaid F, Liu CL, Liu J, Tordjman J, Clement K, Lee CH, Hotamisligil GS, Libby P, and Shi GP. 2015. Leptin Deficiency Shifts Mast Cells toward Anti-Inflammatory Actions and Protects Mice from Obesity and Diabetes by Polarizing M2 Macrophages. Cell Metab. 22: 1045–1058. [PubMed: 26481668]
34. Pérez-Pérez A, Vilariño-García T, Fernández-Riejos P, Martín-González J, Segura-Egea JJ, and Sánchez-Margalet V. 2017. Role of leptin as a link between metabolism and the immune system. Cytokine Growth Factor Rev. 35: 71–84. [PubMed: 28285098]
35. Francisco V, Pino J, Campos-Cabaleiro V, Ruiz-Fernández C, Mera A, Gonzalez-Gay MA, Gómez R, and Gualillo O. 2018. Obesity, fat mass and immune system: Role for leptin. Front. Physiol 9: 1–20. [PubMed: 29377031]
36. Battle M, Gillespie C, Quarshie A, Lanier V, Harmon T, Wilson K, Torroella-Kouri M, and Gonzalez-Perez RR. 2014. Obesity induced a leptin-Notch signaling axis in breast cancer. Int. J. Cancer 134: 1605–1616. [PubMed: 24114531]

37. Rondini E, Harvey A, Steibel J, Hursting S, and Fenton J. 2011. Energy Balance Modulates Colon Tumor Growth: Interactive Roles of Insulin and Estrogen. Mol. Carcinog 50: 370–382. [PubMed: 21480390]

38. Seoane-Collazo P, Martínez-Sánchez N, Milbank E, and Contreras C. 2020. Incendiary leptin. Nutrients 12: 1–34.

39. Hwang S, Kwon A-Y, Jeong J-Y, Kim S, Kang H, Park J, Kim J-H, Han OJ, Lim SM, and An HJ. 2020. Immune gene signatures for predicting durable clinical benefit of anti-PD-1 immunotherapy in patients with non-small cell lung cancer. Sci. Rep 10: 643. [PubMed: 31959763]

40. Williams CB, Yeh ES, and Soloff AC. 2016. Tumor-associated macrophages: unwitting accomplices in breast cancer malignancy. npj Breast Cancer 2: 15025. [PubMed: 26998515]

41. Mancuso P 2016. The role of adipokines in chronic inflammation. ImmunoTargets Ther. 5: 47–56. [PubMed: 27529061]

42. Jiang X, Wang J, Deng X, Xiong F, Ge J, Xiang B, Wu X, Ma J, Zhou M, Li X, Li Y, Li G, Xiong W, Guo C, and Zeng Z. 2019. Role of the tumor microenvironment in PD-L1/PD-1-mediated tumor immune escape. Mol. Cancer 18: 1–17. [PubMed: 30609930]

43. Rivadeneira DB, DePeaux K, Wang Y, Kulkarni A, Tabib T, Menk AV, Sampath P, Lafyatis R, Ferris RL, Sarkar SN, Thorne SH, and Delgoffe GM. 2019. Oncolytic Viruses Engineered to Enforce Leptin Expression Reprogram Tumor-Infiltrating T Cell Metabolism and Promote Tumor Clearance. Immunity 51: 548–560.e4. [PubMed: 31471106]

44. Chan JL, Bullen J, Stoyneva V, DePaoli AM, Addy C, and Mantzoros CS. 2005. Recombinant Methionyl Human Leptin Administration to Achieve High Physiologic or Pharmacologic Leptin Levels Does Not Alter Circulating Inflammatory Marker Levels in Humans with Leptin Sufficiency or Excess. J. Clin. Endocrinol. Metab 90: 1618–1624. [PubMed: 15613407]

45. Huang H, Zhang J, Ling F, Huang Y, Yang M, Zhang Y, Wei Y, Zhang Q, Wang H, Song L, Wu Y, Yang J, and Tang J. 2021. Leptin Receptor (LEPR) promotes proliferation, migration, and invasion and inhibits apoptosis in hepatocellular carcinoma by regulating ANXA7. Cancer Cell Int. 21: 4. [PubMed: 33397392]

Key Points

- Obesity enhances tumor growth while priming macrophage for inflammatory phenotypes.
- The obesity-associated hormone leptin is sufficient to enhance anti-tumor immunity.
- Leptin reprograms macrophages to complement PD-1 blockade immunotherapy.

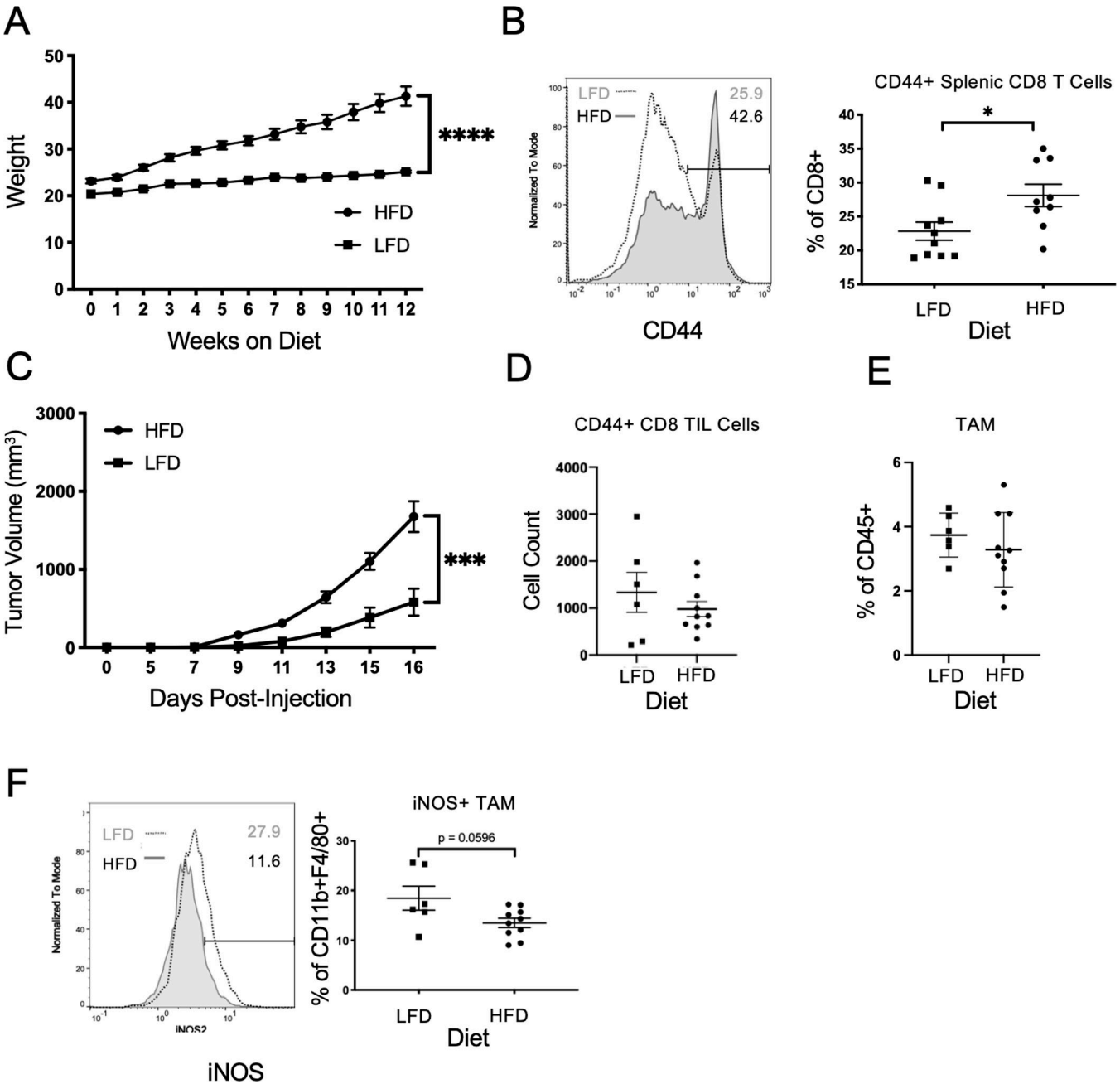

Figure 1. Obesity increases tumor growth and decreases anti-tumor inflammation

A. Five-week old C57BL/6 male mice were maintained on a control standard chow diet (n=8) or 60% kcal from fat high-fat diet (n=8) for 12 weeks and body weight was measured weekly. Two-way ANOVA with Tukey post-hoc test *p* values used. **B.** Spleens from mice on their respective diet for 12 weeks were processed into single cell suspensions and were analyzed by flow cytometry for cytotoxic T cells. Representative histogram of mean fluorescence intensity (MFI), and frequency of $CD44^+$ splenic $CD8^+$ T cells following diet treatment. **C**. C57BL/6 male mice on a control standard chow diet (n=10) or 60 kcal high-fat diet (n=10) for 12 weeks were injected subcutaneously with 10^5 MC38-CEA1 cells in

the right flank. Tumor growth over time measured by digital calipers for 16 days. Tumor volume calculated as (length x width^2)/2. Tumors from mice with MC38-CEA1 tumors were collected 16 days post-injection and were processed into single cell suspensions before flow cytometric analysis. **D.** Absolute cell count of CD44$^+$ cytotoxic CD8$^+$ tumor-infiltrating lymphocytes (TILs) from LFD tumors (n=8) and HFD tumors (n=8). **E.** Frequency of CD11b$^+$F4/80$^+$Tumor-Associated Macrophages following diet treatment. **F.** Representative histogram of mean fluorescence intensity and frequency of iNOS$^+$ TAMs following diet treatment. Two-tailed Mann Whitney test *p* values shown. *$p < 0.05$; ***$p < 0.001$; ****$p < 0.0001$; ns, not significant.

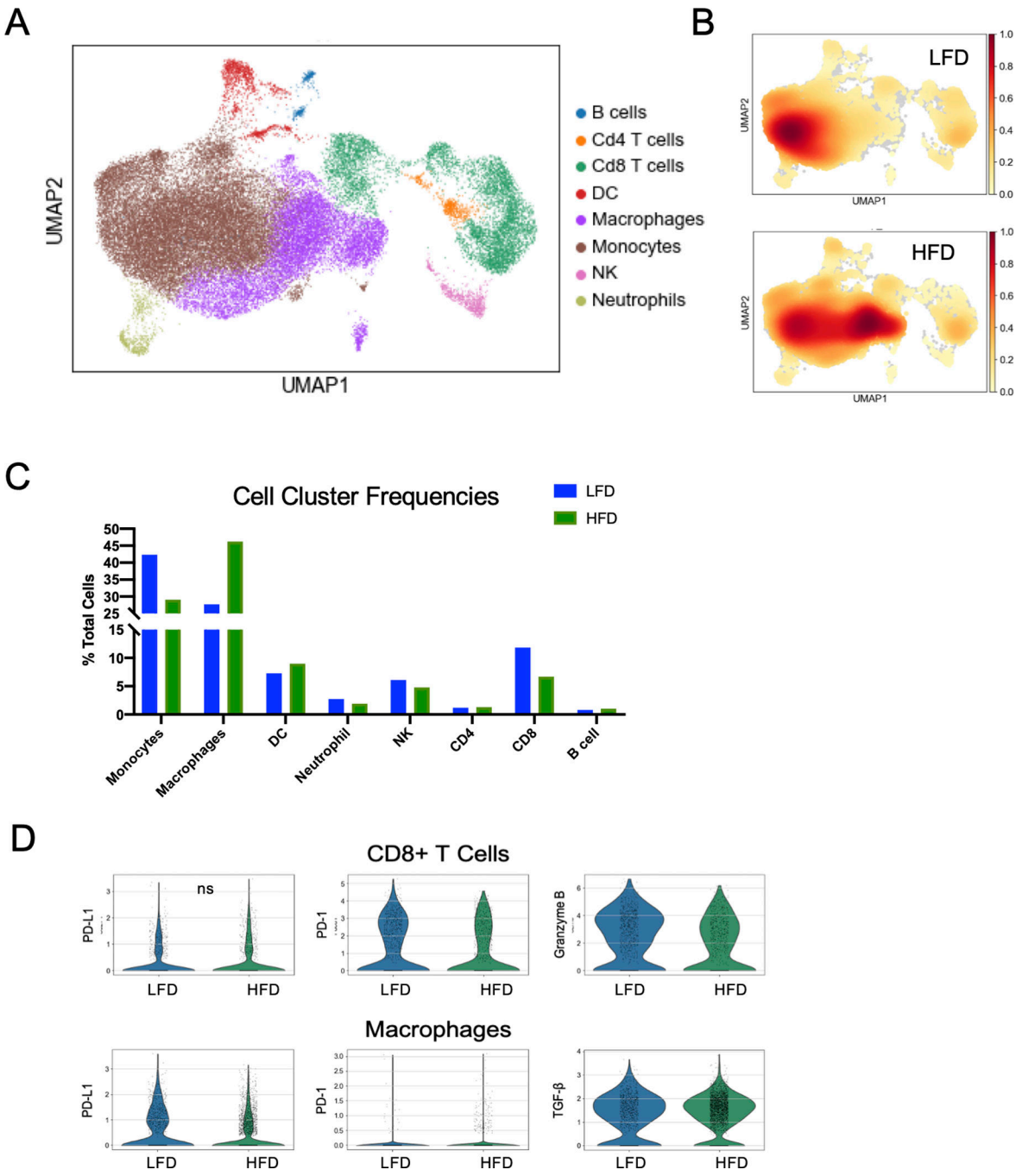

Figure 2. Obesity alters tumor immune cell landscape

A. UMAP plot with SingleR desgnations from single-cell RNA sequencing of CD45^{+} sorted intratumoral cells from lean and obese mice with subcutaneous MC38 tumors (3 tumors from each diet were pooled together in equal number of live cells). **B**. Density Gradient UMAP plots for LFD and HFD intratumoral cells. **C.** Frequency of singleR designated immune cell subtypes within respective diet. **D.** Violin Plots of Single cell gene expression of CD8^{+} T Cells and macrophages from CD45^{+} intratumoral cells in LFD and HFD

treatments. Lack of statistical significance is indicated by “ns” while the other plots were at least $p<0.05$ significant following corrections.

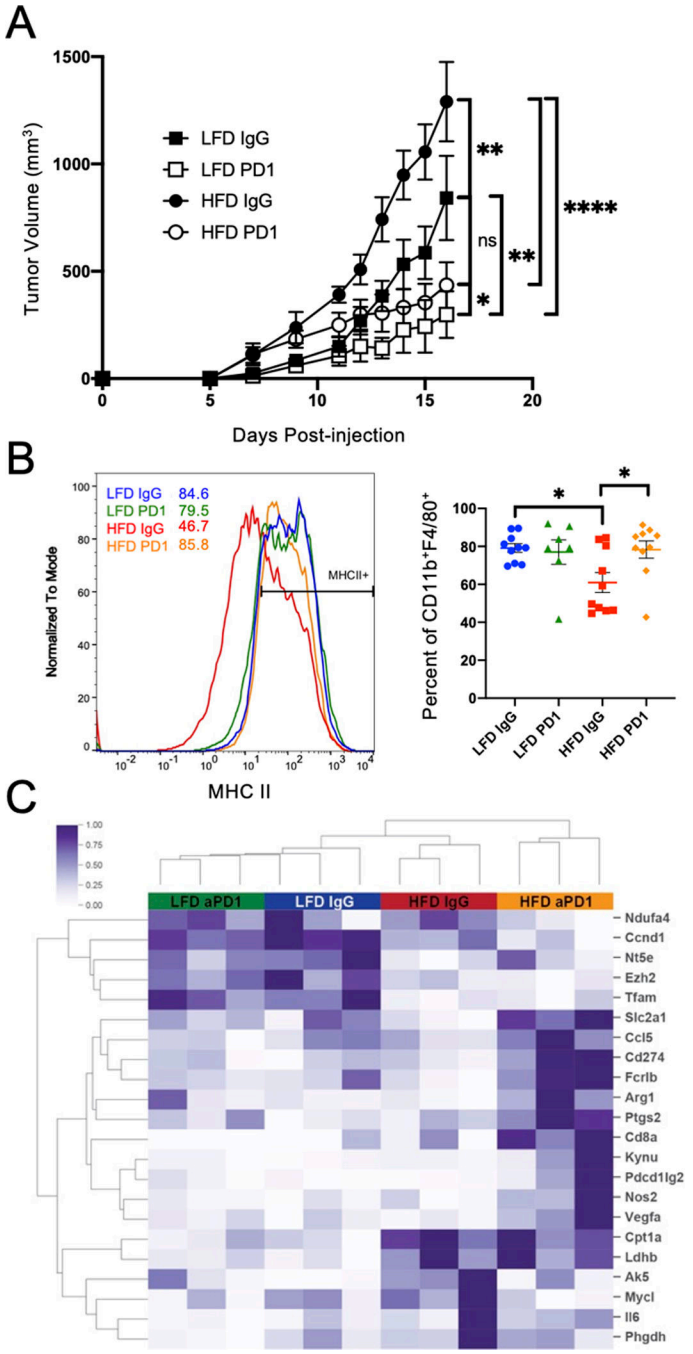

Figure 3. Tumor-associated macrophages repolarize in diet-induced obese anti-PD-1 treated mice

A. Tumor volume calculations over time following subcutaneous injeciton of 2.5×10^5 MC38-CEA1 cells in the right flank in C57BL/6 male mice fed a control standard chow diet (n=10) or 60 kcal high-fat diet (n=10) for 12 weeks. On day 5 post tumor cell-injection, mice were injected with either 200 μg IgG control antibody or anti-PD-1 antibody. The injections continued every two days until tumors were collected on day 16 post-injection. Tumor volume calculated as (length x width^2)/2. Two-way ANOVA with Tukey post-hoc test *p* values were used. **B.** MC38-CEA1 tumors from LFD IgG (n=10), LFD PD1 (n=10), HFD

IgG (n=10), and HFD PD1 (n=10) mice collected 16 days post-injection were processed into single cell suspensions. Representative histogram of MFI and frequency of $MHCII^+$ on $CD11b^+F4/80^+$ TAMs measured by flow cytometry from LFD IgG (n=10), LFD PD1 (n=7), HFD IgG (n=10), and HFD PD1 (n=10). **C.** Unsupervised cluster analysis of differentially expressed metabolic mRNA transcripts from Nanostring analysis of sorted live $CD45^+$ $CD11b^+$ $F4/80^{hi}$ $Ly6G^-$ $Ly6C^{lo}$ $CD3^-$ $CD19^-$ $NKp46^-$ macrophages from MC38 tumor suspensions (n=3). Data are shown as mean± S.E.M., with all individual points shown. Ordinary one-way ANOVA test p values shown. *$p < 0.05$; **$p < 0.01$; ****$p < 0.0001$; ns, not significant.

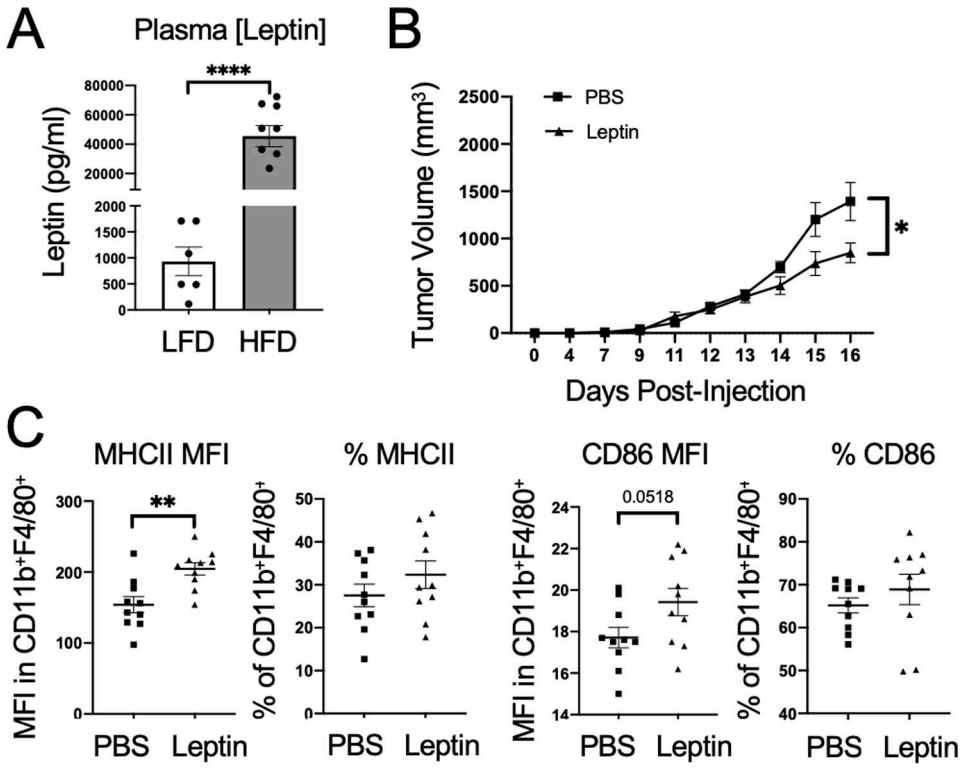

Figure 4. Leptin decreases tumor growth and promotes TAM repolarization

A. Plasma collected from MC38-CEA1 tumor-bearing C57BL/6 male mice on a control standard chow diet (n=6) or 60 kcal high-fat diet (n=8) was measured for leptin by ELISA. Two-tailed Mann Whitney test *p* values shown. **B.** Five-week old C57BL/6 male mice on a control standard chow diet were injected with either 200 μL of leptin (1 μg/g body weight) or PBS control twice a day for two weeks before subcutaneous injections with 10^5 MC38-CEA1 cells were given in the right flank. Leptin injections continued twice daily throughout the tumor growth period. MC38-CEA1 tumor volume over time of PBS or leptin-treated mice measured using digital caliper. Two-way ANOVA with Tukey post-hoc test *p* values used. **C.** MFI and corresponding frequency of MHCII and CD86 expression on $CD11b^+$ and $F480^+$ TAMs. Data are shown as mean± S.E.M., with all individual points shown. Two-tailed Mann Whitney test *p* values shown. $*p < 0.05$; $**p < 0.01$; $***p < 0.001$.

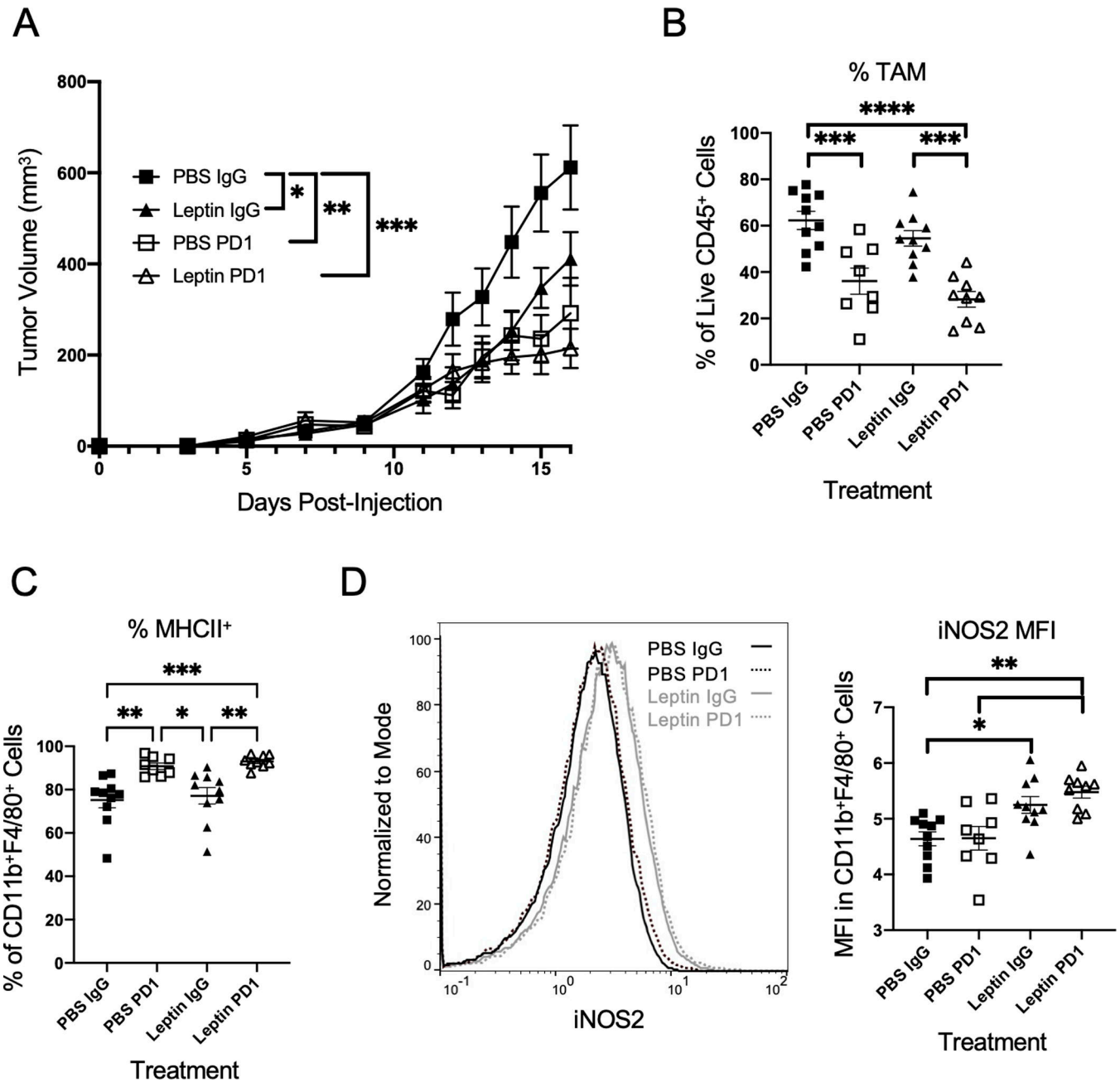

Figure 5. Acute leptin treatments cooperate with PD1 blockade immunotherapy and repolarize TAMs to M1-like phenotypes

Five-week old C57BL/6 male mice were given subcutaneous injections with 2.5×10^5 MC38-CEA1 cells in the right flank. On day 5 post tumor-injection, mice were injected with either 200 μg IgG control antibody or αPD-1 antibody, and the injections continued every two days. Additionally, on day 5 post-tumor injection, mice received either leptin (1 μg/g body weight) or PBS control twice a day. **A**. Tumor volume over time for the PBS IgG antibody (n=10), Leptin IgG antibody (n=10), PBS + anti-PD-1 antibody (n=10), and Leptin + anti-PD-1 antibody continued until 16 days post-injection. Two-way ANOVA with Tukey post-hoc test *p* values used. **B.** Frequency of $CD11b^+$ and $F4/80^+$ TAMs. **C.** Frequency of

MHCII^{+} TAMs. **D.** Representative histogram and corresponding MFI expression of iNOS2 in TAMs. Two-tailed Mann Whitney test p values shown. *$p < 0.05$; **$p < 0.01$; ***$p < 0.001$, ****$p < 0.0001$.